2015

Wavelength Dependent Specific Plasmon Resonance Coupling of Single Silver Nanoparticles with EGFP

Kerry J. Lee
Old Dominion University

Tao Huang
Old Dominion University

Prakash D. Nallathamby
Old Dominion University

Original Publication Citation

Lee, K. J., Huang, T., Nallathamby, P. D., & Xu, X. H. N. (2015). Wavelength dependent specific plasmon resonance coupling of single silver nanoparticles with EGFP. *Nanoscale, 7*(42), 17623-17630. doi:10.1039/c5nr05234c

HHS Public Access

Author manuscript

Nanoscale. Author manuscript; available in PMC 2016 November 14.

Published in final edited form as:

Nanoscale. 2015 November 14; 7(42): 17623–17630. doi:10.1039/c5nr05234c.

Wavelength Dependent Specific Plasmon Resonance Coupling of Single Silver Nanoparticles with EGFP

Kerry J. Lee, **Tao Huang**, **Prakash D. Nallathamby**, and **Xiao-Hong Nancy Xu***

Department of Chemistry and Biochemistry, Old Dominion University, Norfolk, VA 23529

Abstract

Noble metal nanoparticles (NPs) possess unique plasmonics properties, enabling them to serve as sub-diffraction light sources and nano antenna for a wide range of applications. Here we report specific interaction of single Ag NPs with single EGFP molecules and high dependence of their interaction upon localized-surface-plasmon-resonance (LSPR) spectra of single Ag NPs and EGFP. LSPR spectra of single red Ag NPs show a stunning 60-nm blue-shift during their incubation with EGFP, whereas they remain unchanged during their incubation with bovine serum albumin (BSA). Interestingly, the peak wavelengths of LSPR spectra of green and blue Ag NPs remain essentially unchanged. These interesting findings suggest that plasmon-resonance-energy-transfer (PRET) from single Ag NPs to EGFP might follow a two-photon excitation mechanism to excite EGFP and fluorescence of excited EGFP might couple with plasmon of single NPs that lead to the blue-shift of the red NPs. These distinctive phenomena are only observed by real-time single NP spectroscopic measurements. This study offers exciting new opportunities to design new sensing and imaging tools with high specificity and sensitivity to study long-range molecular interactions and dynamic events in single live cells, and to probe underlying molecular mechanisms of PRET.

Keywords

Silver nanoparticles; localized surface plasmon resonance spectra of single nanoparticles; EGFP-nanoparticle interaction; electromagnetic coupling; plasmon resonance energy transfer

Introduction

Noble metal nanoparticles (e.g., silver nanoparticle, Ag NPs) possess distinctive plasmonics properties.[1, 2] The NPs can scatter and absorb incident light very efficiently at a given resonance wavelength, leading to an enhanced electromagnetic near-field on the NP, and enabling them to serve as nanoscale energy transfer antenna for a wide range of applications from design of nanophotonic and photovoltaic devices to biological sensing and imaging.[3–13] The coupling of the enhanced electromagnetic field on single Ag NPs with nearby excited states of fluorophore offers an important model to study nanoscale energy transfer for better understanding of their fundamental mechanisms and study of long-range

*To whom correspondence should be addressed: xhxu@odu.edu; www.odu.edu/sci/xu/xu.htm; Tel/fax: (757) 683-5698.

molecular interactions, far beyond 10 nm distance limited by F_rster resonance energy transfer (FRET).[6, 8]

The localized surface plasmon resonance (LSPR) spectra of single NPs highly depend upon their sizes, shapes, surface properties, and surrounding environments.[1, 214, 15] These unique optical properties enable them to serve as single molecule nanoparticle optical biosensors (SMNOBS) for molecular analysis of biomarkers of interest, and as photostable optical imaging probes for real-time imaging of single live cells and embryos.[3, 5, 7, 9, 16–19] Fluorescence proteins (e.g., GFP, YFP, RFP) have been widely used as effective optical probes for real-time study of proteins expressed in live cells and *in vivo*.[20–23] Therefore, study of interaction of Ag NPs with GPF offers the possibility of using NPs for the study of long-range protein-protein interactions and determining their roles in cellular functions in single live cells *in vivo* in real time, as well as better understanding of underlying molecular mechanisms of NP-fluorophore interactions.

Current studies primarily focus on the study of plasmonic coupling among metallic NPs, nanomaterial surface energy transfer (NSET) from a excited fluorophore (donor) to a metallic NP (acceptor) via dipole-surface energy transfer, and quenching or enhancing effects of metallic NPs on the fluorescence emission of their nearby excited fluorophore.[6, 8, 24–31] A few studies have reported the use of LSPR of the gold (Au) NPs to excite the nearby fluorophore via plasmon resonance energy transfer (PRET) for sensing applications.[6, 8, 24–28] However, the dependence and specificity of PRET upon the LSPR spectra of single NPs, its underlying mechanisms and potential applications remain to be explored. In this study, we investigate the dependence of PRET and interaction of single Ag NPs with single EGFP molecules upon LSPR spectra of single Ag NPs. We found the high dependence of PRET upon the LSPR spectra of single Ag NPs and the stunning blue shift of LSPR spectra of single red Ag NPs in the presence of EGFP.

Results and Discussion

We have synthesized and purified Ag NPs using the approaches described in Methods.[5, 15, 17, 19, 32] We then characterized sizes, shapes and plasmonic optical properties of single Ag NPs using high resolution transmission electron microscopy (HRTEM), and dark-field optical microscopy and spectroscopy (DFOMS) (Figure 1), respectively. TEM image and histogram of size distribution of single Ag NPs in Figure 1A and B show that the majority of NPs are nearly spherical with average diameters of 11.5 ± 2.2 nm, ranging from 6 to 20 nm, and a few of NPs are dimmer.

A representative optical image of single Ag NPs shows that the majority of NPs are blue with some being green and a few red (Figure 1C). We acquired and analyzed 20 images similar to those in Figure 1C and found that the NP solution has 76.9% of blue NPs, 17.3% green NPs and 5.8% of red NPs. The LSPR spectra of representative single blue, green and red NPs show peak wavelengths (full-width-at-half-maximum), λ_{max} (FWHM), of 490 nm (58 nm), 536 nm (74 nm), and 620 nm (70 nm), respectively (Figure 1D). Notably, similar high heterogeneity of LSPR spectra of single NPs was also observed in our previous studies.[15, 17, 19, 32] LSPR spectra of some of single NPs show longer wavelength than those

of the spherical Ag NPs with the diameters of 6–20 nm, suggesting that some of NPs might have high aspect ratios, rough surfaces or larger diameters and they have gone undetected by TEM. The high heterogeneity of LSPR spectra of single Ag NPs shows high dependence of LSPR spectra of single NPs upon surface properties and shapes (rough surface) of NPs. The correlation between the distribution of sizes and LSPR spectra of single NPs suggests that the dimmer NPs are likely to be plasmonic red NPs. Like the sizes, the shapes and surface roughness of NPs could also contribute significantly to the large distribution of LSPR spectra of single NPs, underscoring the importance of study of LSPR spectra of single NPs. The results further demonstrates the powerful high-throughput detection capability and sensitivity of DFOMS to identify and characterize a very few individual NPs in a mix population of NPs in solution *in situ* and in real time.

We used the molar concentration of single NPs to control the molar ratio of NPs to EGFP as one (one EGFP molecule per NP). Molar concentrations of single NPs (but not atoms or ions) are defined by dividing moles of NPs (number of NP/Avogadro constant) by solution volume.[13, 16, 17, 19, 33, 34] Molar concentration of the NPs is proportional to the number and surface area and properties of individual NPs, which enables the study of surface dependent effects of the NPs on their interaction with EGFP.

The UV-vis absorption spectra of Ag NPs incubated with one molar ratio of EGFP in the PBS buffer for 3 h (Figure 2A) show a red-shift of its peak wavelength from 398 nm to 410 nm. The control experiment shows that the peak wavelength of UV-vis absorption spectra of the Ag NPs incubated with the BSA in the PBS for 3 h remain unchanged at 398 nm (Figure 2B). The result suggests that the interaction of the Ag NPs with the EGFP (fluorophore) and the coupling of absorption of Ag NPs and EGFP most likely play the role of larger red shift of plasmonic absorption spectra of the Ag NPs.

We also investigated the effect of the Ag NPs upon the fluorescence spectra of EGFP using a fluorescence spectrophotometer. Interestingly, the fluorescence excitation and emission spectra of EGFP in the absence and presence of Ag NPs for solution in Figure 2A remain unchanged as shown in Figure 2C and 2D. The result would have suggested that the presence of such low concentration of Ag NPs did not significantly affect the fluorescence spectra of EGFP.

To overcome potential drawbacks of ensemble measurements and to study scattering of plasmon resonance coupling of single Ag NPs with EGFP, we determined the dependence of effects of EGFP on LSPR spectra of single Ag NPs upon the wavelength of LSPR spectra of the NPs using our DFOMS. We added the Ag NP solution into a micro-chamber and allowed a few of single Ag NPs settled on a glass microscope slide. We imaged and acquired LSPR spectra of single Ag NPs on the slides that well represent those in the solution. We then added EGFP solution into the NP solution in the chamber to have one molar ratio of EGFP to NP, and followed the change of LSPR spectra of the same single NPs in real time using DFOMS, as the NPs were incubated with EGFP over time.

For single red NPs with the peak wavelength of LSPR spectra much longer than fluorescence emission of EGFP, we observed a stunning blue-shift of LSPR spectra of the

NPs upon their incubation with EGFP over time (Figure 3). The representative red NP with peak wavelength of LSPR spectra of 657 nm is blue-shifted to 599 nm, gradually changing its color from red to orange upon its incubation with EGFP over 3 h (Figure 3A–B). Its scattering intensity remains essentially unchanged. The other representative red NP with peak wavelength of LSPR spectra of 613 nm is blue-shifted to 553 nm, changing its color from red to yellow/green during its incubation with EGFP over 3 h (Figure 3C–D). Its scattering intensity decreases gradually.

On the contrary, the green NP with peak wavelength of LSPR spectrum of 527 nm remains essentially unchanged during its incubation with EGFP over 3 h (Figure 4A–B). The blue NP with peak wavelength of LSPR spectra of 493 nm also remains essentially unchanged upon its incubation with EGFP over 3 h (Figure 4C–D).

Control experiments were carried out the exactly same way as the study of Ag NPs with EGFP, but replacing EGFP with BSA. The plasmonic color and peak-wavelength of LSPR spectra of single red NPs incubated with BSA over 3 h remain essentially unchanged at 643 nm (Figure 5A–B) while its scattering intensity decreases over time, which could be attributed to the decrease of its dielectric constant and refractivity due to the adsorption of BSA on the surface of NPs. The plasmonic color and peak-wavelength of LSPR spectra of single green NPs incubated with BSA over 3 h also remain essentially unchanged at 528 nm (Figure 5C–D) while its scattering intensity decreases over time, which could be attributed to the decrease of its dielectric constant and refractivity due to the adsorption of BSA on the surface of NPs. Though change of dielectric constant and refractivity of the NPs could lead to the red shift of LSPR spectra of the NPs, these NPs are fairly large with the surface-area-to-volume ratio smaller than 0.5, and their LSPR spectra are less sensitive to the change of dielectric constant and refractivity than smaller NPs (2 nm in diameter with the surface-area-to-volume ratio great than 2). Furthermore, BSA concentration is quite low (0.69 nM) and one molar ratio of BSA to the NP is used. Thus, we did not observe significant shift of LSPR spectra of the NPs as they were exposed to BSA over time.

Unlike EGFP, BSA is not a fluorescence protein and cannot generate fluorescence emission within a visible wavelength (400–800 nm). This control experiment enables us to determine that the fluorescence property of EGFP (but not adsorption of EGFP onto the NPs) plays a leading role in the blue-shift of LSPR spectra of single red NPs. It is most likely that the EGFP were excited by plasmon of NPs, and fluorescence emission of the EGFP was coupled with plasmon resonance of the NPs, which led to the blue shift of LSPR spectra of the red NPs. Furthermore, LSPR spectra of green and blue NPs with peak wavelength at 506–536 and 466–494 nm appear not to provide sufficient energy to excite EGFP or the fluorescence emission of EGFP unable to couple with their plasmon resonance (Table I). Thus, the LSPR spectra of green and blue NPs remain essentially unchanged during their incubation with the EGFP.

We have acquired LSPR spectra of single NPs simultaneously (similar to Figure 1C) as they were exposed to EGFP or BSA over 3 h. Each experiment was repeated three times. The NP solution includes 76.9% of blue NPs, 17.3% green NPs and 5.8% of red NPs. Thus, we have studied at least 92 individual blue NPs, 21 green NPs and 7 red NPs. The results of the

representative three NPs (a-c) of each color are summarized in Table I, which indicates that LSPR spectra of single red NPs show the significant blue shift upon their exposure to EGFP over 3 h, while the LSPR spectra of single blue and green NPs remain essentially unchanged.

Taken together, the results in Figures 4 and 5 and Table I show the high dependence of plasmonic coupling of single Ag NPs with EGFP upon the wavelength of LSPR spectra of the NPs. Further studies are needed to determine its underlying mechanism. Nonetheless, the stunning blue-shift of LSPR spectra of single red NPs by EGFP suggests that PRET from the NP to EGFP might follow a two-photon excitation mechanism to excite EGFP, and the excited EGFP molecules could then couple with plasmon resonance of the NP, which could lead to the blue shift of LSPR spectra of the red NPs. On the contrary, the LSPR spectra of single green or blue NPs remain essentially unchanged. These unique plasmon coupling properties with single NP sensitivity are highly specific to LSPR spectra of single NPs and EGFP, offering a powerful tool for one to study the interaction of Ag NPs with specific proteins that are fused with EGFP in single live cells and *in vivo*.

As we demonstrated in our previous studies, single Ag NPs can serve as photostable (non-photobleaching and non-blinking) imaging probes for following the same single molecules and study of dynamic cellular events of the same single live cells over hours.[3, 5, 7, 9, 17–19, 35] On the contrary, EGFP suffers photobleaching and blinking and cannot be used to follow the same molecule and study the same cells over time using fluorescence microscopy and spectroscopy.[20, 36] Therefore, this study offers an exciting new approach to use photostable Ag NPs to track the EGPF fused proteins for the study of dynamic events of interest in single live cells over a long period of time.

In addition to acquiring the LSPR spectra of single Ag NPs, we also acquired the fluorescence spectra of EGFP around the same individual Ag NPs over time. The results in Figure 6A show that in the vicinity of Ag NPs, the fluorescence emission spectra of EGFP become broader and the fluorescence intensity decreases rapidly while its peak wavelength remains similar to those observed in the absence of Ag NPs in Figure 6B. The results show that the Ag NPs indeed quench the fluorescence emission of EGFP on its surface and NPs indeed interact with EGFP.

In summary, we have studied the interaction of single Ag NPs with single EGFP molecules. We found that the effect of EGFP upon the LSPR spectra of single NPs highly depend upon the peak wavelength of LSPR spectra of the NPs, and the LSPR spectra of red NPs show stunning blue-shift (60 nm) during their incubation with EGFP, while they remain essentially unchanged during their incubation with BSA. Interestingly, the peak wavelength of LSPR spectra of green and blue NPs remain essentially unchanged, while their scattering intensity decreases during their incubation with EGFP over time. These interesting findings suggest that PRET from single Ag NPs to EGFP might have followed a two-photon excitation mechanism to excite EGFP and fluorescence of excited EGFP might have coupled with plasmon of single Ag NPs, leading to the blue-shift of the red NPs. These findings offer exciting new approaches to design new sensing and imaging tools with high specificity and sensitivity to study long-range molecular interactions and dynamic events of single live cells

in vivo. Furthermore, these new findings are achieved by single NP measurements, but not ensemble measurements, underscoring the importance of single NP study of plasmon coupling. Further studies are underway to determine their underlying molecular mechanisms and to explore their powerful applications.

Methods

Synthesis and Characterization of Stable and Purified Ag NPs

We synthesized and characterized the Ag NPs (11.5 ± 2.2 nm) using the similar approaches as we described previously.[15, 17, 19, 32] We mixed $AgClO_4$ (0.1 mM in deionized (DI) water) with a freshly prepared ice-cold solution of sodium citrate (3 mM) and sodium borohydride (10 mM) under stirring overnight to synthesize the NPs. We filtered the NP solution using a 0.22 μm filter and washed the NPs three times with DI water using centrifugation to remove the chemicals involved in NP synthesis, and resuspended the NPs in DI water. The washed Ag NPs are very stable (non-aggregated) in DI water for months and remain stable in PBS buffer (0.5 mM phosphate buffer, 1.5 mM NaCl at pH 7.0) throughout their incubation with EGFP over 3 h.

We characterized the concentrations, optical properties, and sizes of NPs using UV-vis spectroscopy (Hitachi U-2010), dark-field optical microscopy and spectroscopy (DFOMS), dynamic light scattering (DLS), and high-resolution transmission electron microscopy (HR-TEM) (JEOL, JEM-2100F), respectively.[11, 16, 17, 37] We have fully described the design and construction of our DFOMS in our previous studies for real-time imaging and spectroscopic characterization of single NPs in solutions, single live cells and single embryos, and for single molecule detection.[3, 5, 7, 9, 11, 13, 15–19, 21, 32–34, 38, 39] In this study, we used dark-field microscope equipped with Multispectral Imaging System (MSIS, N-MSI-VIS-FLEX, CRi, Hopkiton, MA) to image and characterize LSPR spectra of single Ag NPs. The MSIS is an integrated system of a CCD camera (SonyICX 285) and liquid-crystal-tunable-filter. The dark-field microscope consists of a dark-field condenser (oil, 1.43–1.20), a microscope illuminator (Halogen lamp, 100 W), and a 100× objective (Plan fluor 100×, N.A. 0.5–1.3, oil). All chemicals and reagents, except EGFP (BioVision, Mountain View, CA), were purchased from Sigma and used as received. We used the nanopure DI water (18 MΩ, Barnstead) to prepare solutions and rinse glassware.

Ensemble Study of Effect of EGFP on Plasmonic Absorption Spectra of Ag NPs and Effects of Ag NPs on Fluorescence Emission of EGFP

We acquired UV-vis absorption spectra of Ag NPs (0.69 nM) alone, BSA (0.69 nM) alone, EGFP (0.69 nM) alone, and Ag NPs (0.69 nM) incubated with EGFP (0.69 nM) or BSA (0.69 nM) in the PBS buffer over 3 h. We acquired fluorescence excitation and emission spectra of EGFP (0.69 nM) alone, Ag NPs (0.69 nM) alone, and EGFP (0.69 nM) incubated with Ag NPs (0.69 nM) in the PBS buffer using a fluorescence spectrometer (Perkin-Elmer LS50B).

Single NP Study of Effect of EGFP on LSPR Spectra of Single Ag NPs and Quenching Effect of Single Ag NPs on Fluorescence Emission of EGFP

The Ag NP solution (0.69 nM in PBS buffer) was added into a sealed micro-chamber. LSPR images and spectra of representative single NPs on the surface of microscope glass cover slide in the chamber were acquired in real-time using DFOMS. EGFP were then injected into the Ag NP solution in the chamber to have the final concentration of EGFP and Ag NPs of 0.69 nM each (one molar ratio). LSPR images and spectra of single NPs and fluorescence images and spectra of EGPF around single NPs were acquired at every 30 min over their incubation of 3 h using DFOMS and fluorescence microscopy and spectroscopy (Nikon E-600) equipped with MSIS, respectively.

Acknowledgments

This work is supported in part by NSF (CBET 0507036 and CBET 1450936) and NIH (R01 GM0764401). Lee and Nallathamby are grateful for the support of NSF-GRAS (CBET 0541661) and Dominion Scholar Fellowship, respectively.

References

1. Kreibig, U.; Vollmer, M. Optical Properties of Metal Clusters. Springer; Berlin: 1995. p. 14-123.
2. Mie G. Annu Phys. 1908; 25:377–445.
3. Huang T, Browning LM, Xu XHN. Nanoscale. 2012; 4:2797–2812. [PubMed: 22331098]
4. Atwater HA, Polman A. Nat Mater. 2010; 9:205–213. [PubMed: 20168344]
5. Huang T, Nallathamby PD, Gillet D, Xu XHN. Anal Chem. 2007; 79:7708–7718. [PubMed: 17867652]
6. Ray PC, Fan Z, Crouch RA, Sinha SS, Pramanik A. Chem Soc Rev. 2014; 43:6370–6404. and references therein. [PubMed: 24902784]
7. Huang T, Xu XHN. Nanoscale. 2011; 3:3567–3572. [PubMed: 21633732]
8. Kern AM, Zhang D, Brecht M, Chizhik AI, Failla AV, Wackenhut F, Meixner AJ. Chem Soc Rev. 2014; 43:1263–1286. and references therein. [PubMed: 24365864]
9. Huang T, Nallathamby PD, Xu XHN. J Am Chem Soc. 2008; 130:17095–17105. [PubMed: 19053435]
10. Anker JN, Hall WP, Lyandres O, Shah NC, Zhao J, Duyne RP. Nat Mater. 2008; 7:442–453. and references therein. [PubMed: 18497851]
11. Xu XHN, Chen J, Jeffers RB, Kyriacou SV. Nano Lett. 2002; 2:175–182.
12. Jain PK, Huang X, El-Sayed IH, El-Sayed MA. Acc Chem Res. 2008; 41:1578–1586. and references therein. [PubMed: 18447366]
13. Browning LM, Huang T, Xu XHN. Interface Focus. 2013; 3:20120098. [PubMed: 24427540]
14. Kelly KL, Coronado E, Zhao LL, Schatz GC. J Phys Chem B. 2003; 107:668–677. and references therein.
15. Nallathamby PD, Huang T, Xu XHN. Nanoscale. 2010; 2:1715–1722. [PubMed: 20820702]
16. Lee KJ, Nallathamby PD, Browning LM, Desai T, Cherukui P, Xu XHN. Analyst. 2012; 137:2973–2986. [PubMed: 22563577]
17. Lee KJ, Nallathamby PD, Browning LM, Osgood CJ, Xu XHN. ACS Nano. 2007; 1:133–143. [PubMed: 19122772]
18. Nallathamby PD, Lee KJ, Desai T, Xu XHN. Biochemistry. 2010; 49:5942–5953. [PubMed: 20540528]
19. Nallathamby PD, Lee KJ, Xu XHN. ACS Nano. 2008; 2:1371–1380. [PubMed: 19206304]
20. Tsien, RY.; Waggoner, A. Handbook of Biological Confocal Microscopy. 2. Pawley, JB., editor. Plenum; New York: 1995. p. 267-280.

21. Lee KJ, Browning LM, Huang T, Ding F, Nallathamby PD, Xu XHN. Anal Bioanal Chem. 2010; 397:3317–3328. [PubMed: 20544182]
22. Ding F, Lee K, Vahedi-Faridi A, Huang T, Xu XHN. Anal Bioanal Chem. 2011; 400:223–235. [PubMed: 21336797]
23. Ding F, Lee KJ, Vahedi-Faridi A, Yoneyama H, Osgood CJ, Xu XHN. Analyst. 2014; 139:3088–3096. [PubMed: 24781334]
24. Reil F, Hohenester U, Krenn JR, Leitner A. Nano Lett. 2008; 8:4128–4133. [PubMed: 19367798]
25. Reineck P, Gómez D, Ng SH, Karg M, Bell T, Mulvaney P, Bach U. ACS Nano. 2013; 7:6636–6648. [PubMed: 23713513]
26. Shi L, Jing C, Gu Z, Long YT. Sci Rep. 2015:5.
27. Stobiecka M, Hepel M. Phys Chem Chem Phys. 2011; 13:1131–1139. [PubMed: 21072434]
28. Wiener DM, Lionberger TA. Anal Chem. 2013; 85:5095–5102. [PubMed: 23581610]
29. Song Y, Nallathamby PD, Huang T, Elsayled-Ali H, Xu XHN. J Phys Chem C. 2010; 114:74–81.
30. Sonnichsen C, Reinhard BM, Liphardt J, Alivisatos AP. Nat Biotechnol. 2005; 23:741–745. [PubMed: 15908940]
31. Jain PK, El-Sayed MA. Nano letters. 2007; 7:2854–2858. [PubMed: 17676810]
32. Nallathamby PD, Xu XHN. Nanoscale. 2010; 2:942–952. [PubMed: 20648292]
33. Browning LM, Lee KJ, Huang T, Nallathamby PD, Lowman J, Xu XHN. Nanoscale. 2009; 1:138–152. [PubMed: 20644873]
34. Lee KJ, Browning LM, Nallathamby PD, Desai T, Cherukui P, Xu XHN. Chem Res Toxico. 2012; 25:1029–1046.
35. Lee KJ, Browning LM, Nallathamby PD, Xu XHN. Nanoscale. 2013; 5:11625–11636. [PubMed: 24056877]
36. Dickson RM, Cubitt AB, Tsien RY, Moerner WE. Nature. 1997; 388:355–358. [PubMed: 9237752]
37. Lee KJ, Browning LM, Nallathamby PD, Xu XHN. Chem Res Toxicol. 2013; 26:904–917. [PubMed: 23621491]
38. Xu XHN, Brownlow WJ, Kyriacou SV, Wan Q, Viola JJ. Biochemistry. 2004; 43:10400–10413. [PubMed: 15301539]
39. Kyriacou SV, Brownlow WJ, Xu XHN. Biochemistry. 2004; 43:140–147. [PubMed: 14705939]

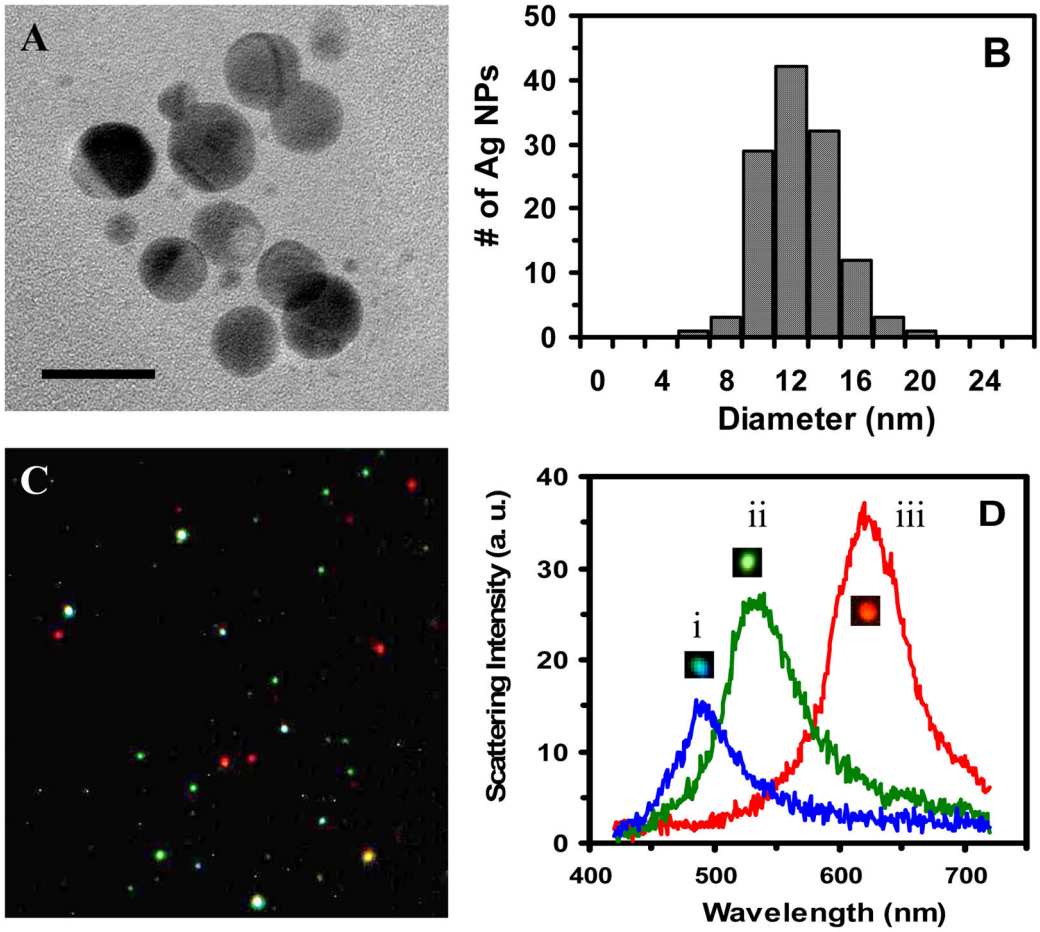

Figure 1. Characterization of sizes, shapes and plasmonic optical properties of single purified Ag NPs in DI water

(A) HRTEM images show that the shapes of majority of NPs are nearly spherical with some being dimmers. The scale bars are 20 nm.

(B) Histogram of size distribution of single NPs determined by HRTEM indicates their average diameters of 11.5 ± 2.2 nm, ranging from 6 to 20 nm.

(C) Dark-field optical images of single NPs in DI water show that the majority of NPs are plasmonic blue with some being green, orange and red.

(D) Representative LSPR spectra of single NPs in (C) show peak wavelengths (full-width-at-half-maximum), λ_{max} (FWHM): (i) 490 (58), (ii) 536 (74), and (iii) 620 (70) nm, for the plasmonic blue, green and red NPs, respectively.

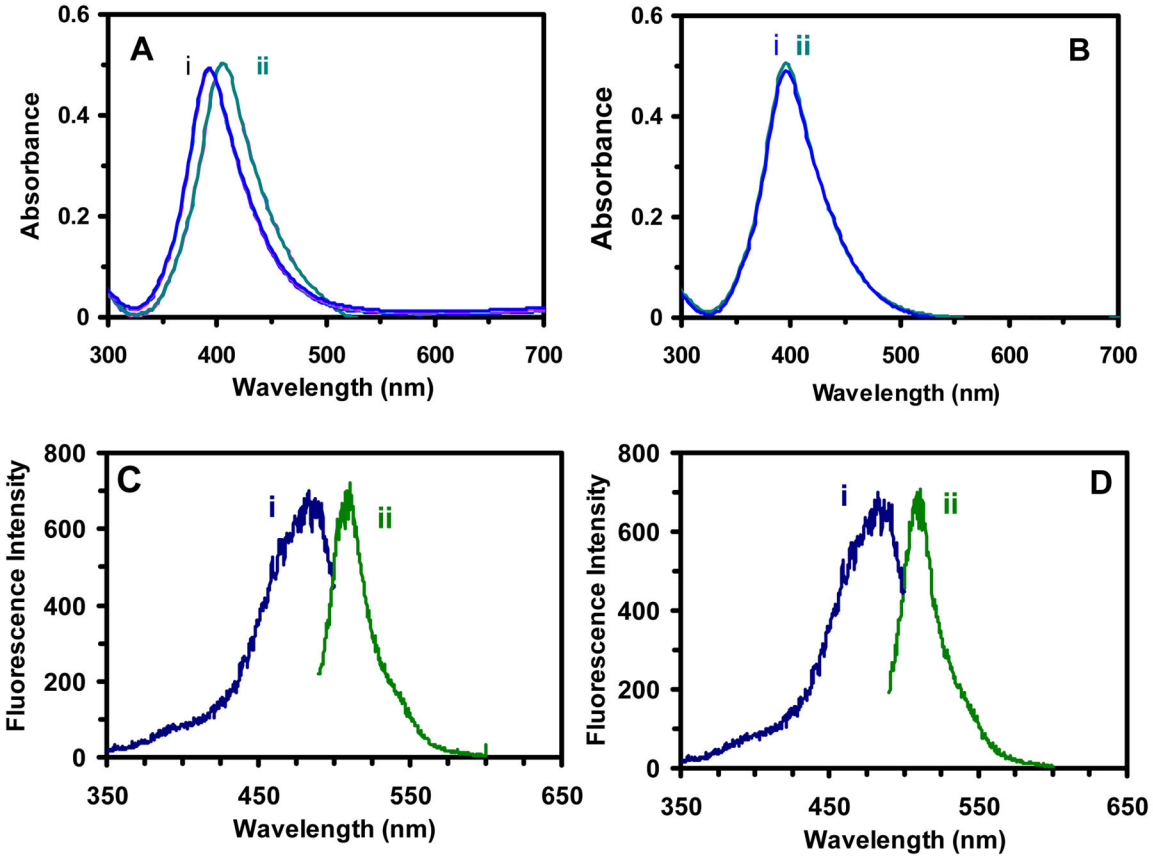

Figure 2.

Study of (A–B) effect of EGFP upon plasmonic absorption spectra of Ag NPs and (C–D) effect of NPs upon fluorescence spectra of EGFP. UV-vis absorption spectra of 0.69 nM Ag NPs in **(A)** show that λ_{max} (FWHM) of the spectrum red-shifts from: (i) 398 nm (58 nm) to (ii) 410 nm (62 nm) in the absence and presence of EGFP (0.69 nM) in the PBS buffer, respectively. UV-vis absorption spectra of 0.69 nM Ag NPs in **(B)** show that λ_{max} (FWHM) of the spectra remain unchanged at (i–ii) 398 nm (58 nm) in the absence and presence of BSA (0.69 nM). (i–ii) Excitation and emission fluorescence spectra of EGFP (0.69 nM) in the PBS buffer: **(C)** in the absence and **(D)** the presence of Ag NPs (0.69 nM), show that λ_{max} (FWHM) of the fluorescence spectra remain unchanged at (i) 483 nm (50 nm) and (ii) 509 nm (25 nm), respectively.

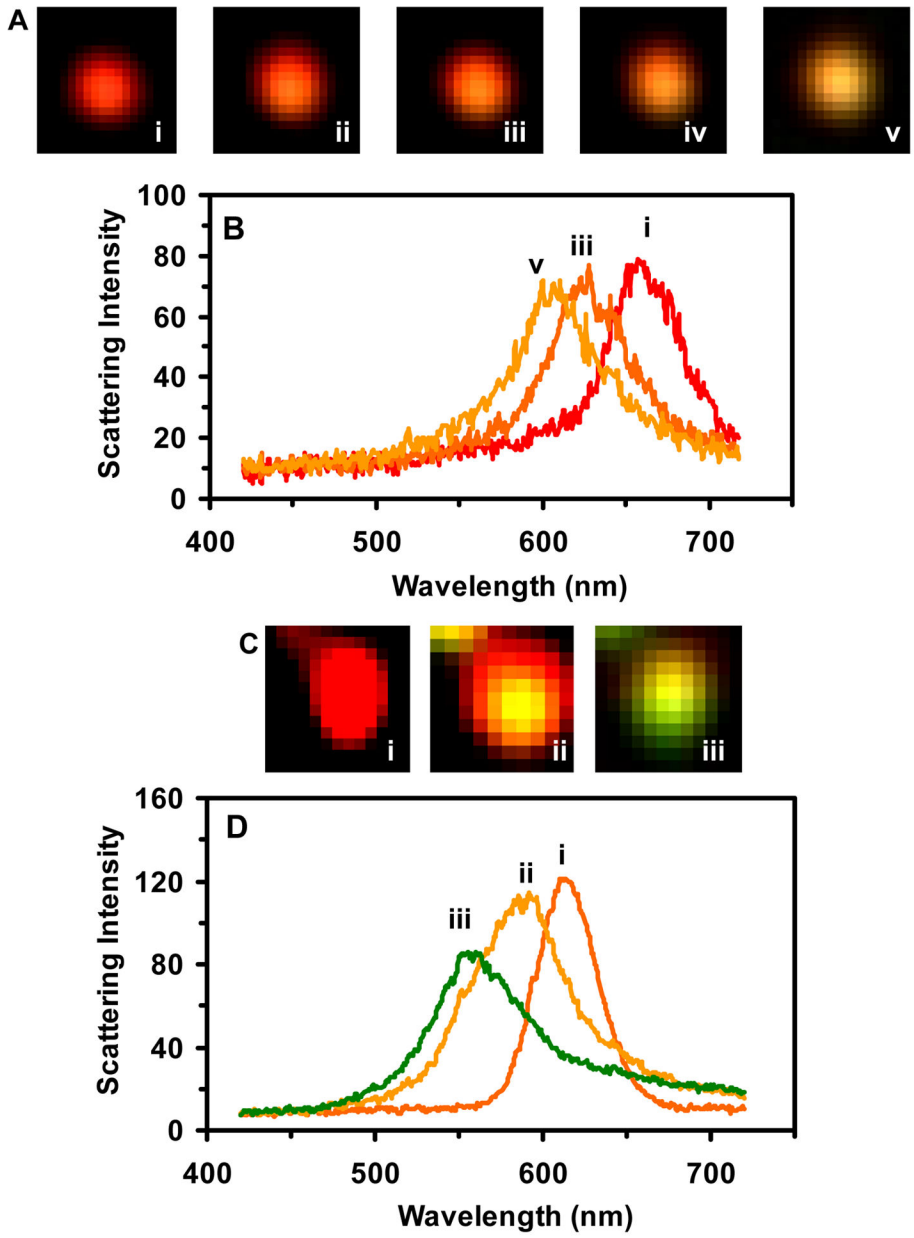

Figure 3.

Significant effect of EGFP upon LSPR spectra of single red Ag NPs with peak wavelength much longer than fluorescence emission peak wavelength of EGFP. **(A–B)** Dark-field optical images and spectra of single red NPs incubated with EGFP in the PBS buffer show blue-shift of λ_{max} from 657 to 599 nm, turning its color from red to orange, over time. **(C–D)** Dark-field optical images and spectra of single red NPs incubated with EGFP in the PBS buffer show blue-shift of λ_{max} from 613 to 553 nm, turning its color from red to yellowish-green, over time. Each image and spectrum was acquired at 30 min interval over 3 h. Representative images and spectra at given time were shown.

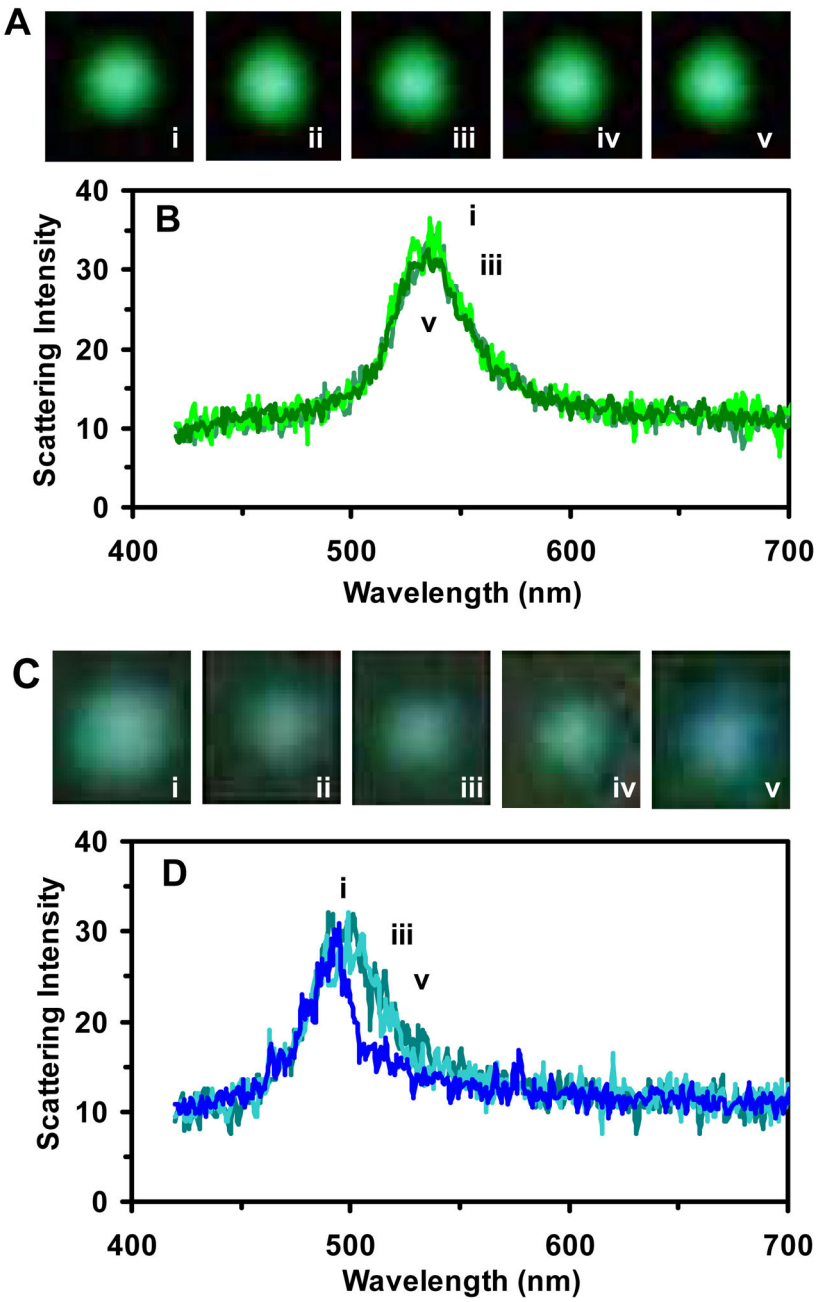

Figure 4.

Little effect of EGFP upon LSPR spectra of single blue and green Ag NPs with peak wavelength close to or shorter than fluorescence emission peak wavelength of EGFP. **(A–B)** Dark-field optical images and spectra of single green Ag NPs incubated with EGFP in the PBS buffer over 3 h show that λ_{max} of 527 nm remain unchanged. **(C–D)** Dark-field optical images and spectra of single blue Ag NPs incubated with EGFP in PBS buffer over 3 h show that λ_{max} of 493 nm remain unchanged.

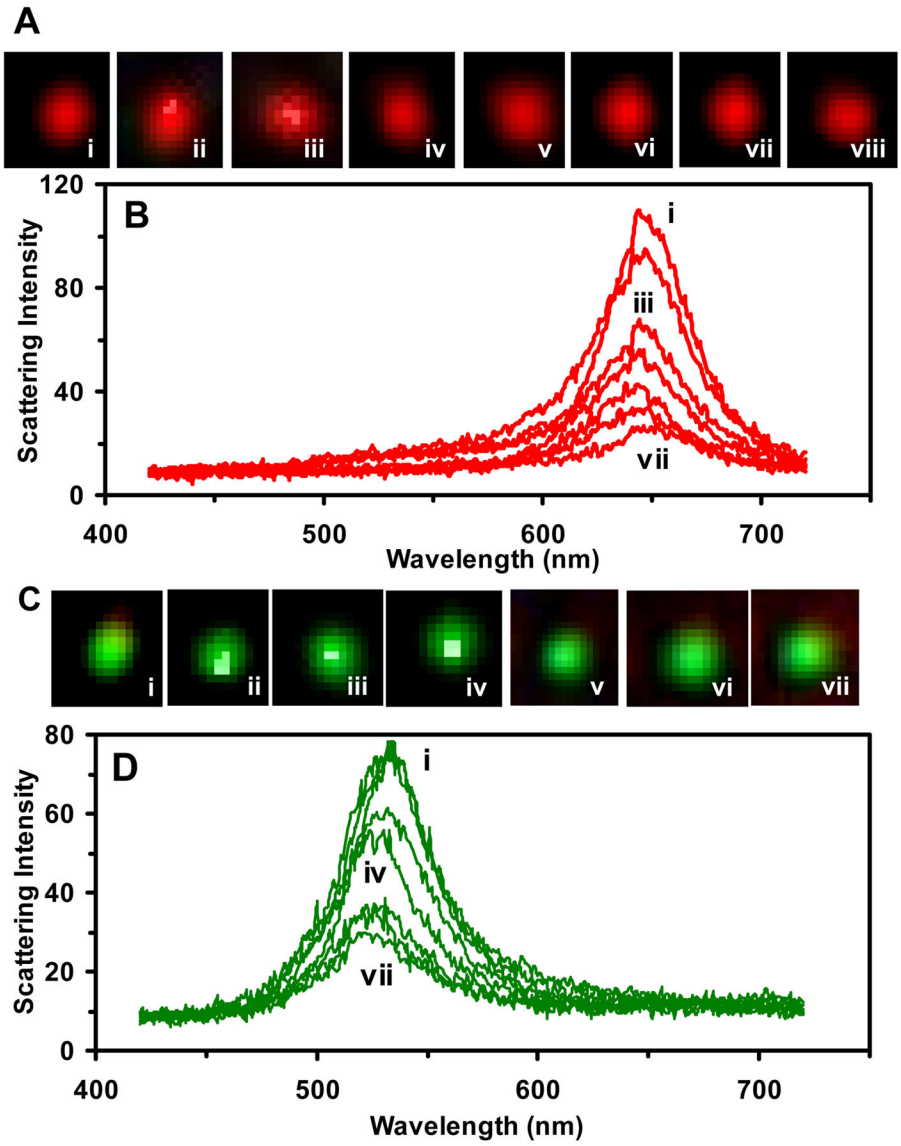

Figure 5.

Control experiments show that the presence of BSA does not affect LSPR spectra of single red and green Ag NPs. **(A–B)** Dark-field optical images and spectra of single red NPs incubated with BSA in the PBS buffer over 3 h show that λ_{max} of the spectrum at 643 nm remain unchanged, while its intensity decreases over time. **(C–D)** Dark-field optical images and spectra of single green NP incubated with BSA in the PBS buffer over 3 h show that λ_{max} of the spectra at 528 nm remain unchanged, while its intensity decreases over time. Each image and spectrum was acquired at 30 min interval over 3 h. Representative images and spectra at given time were shown.

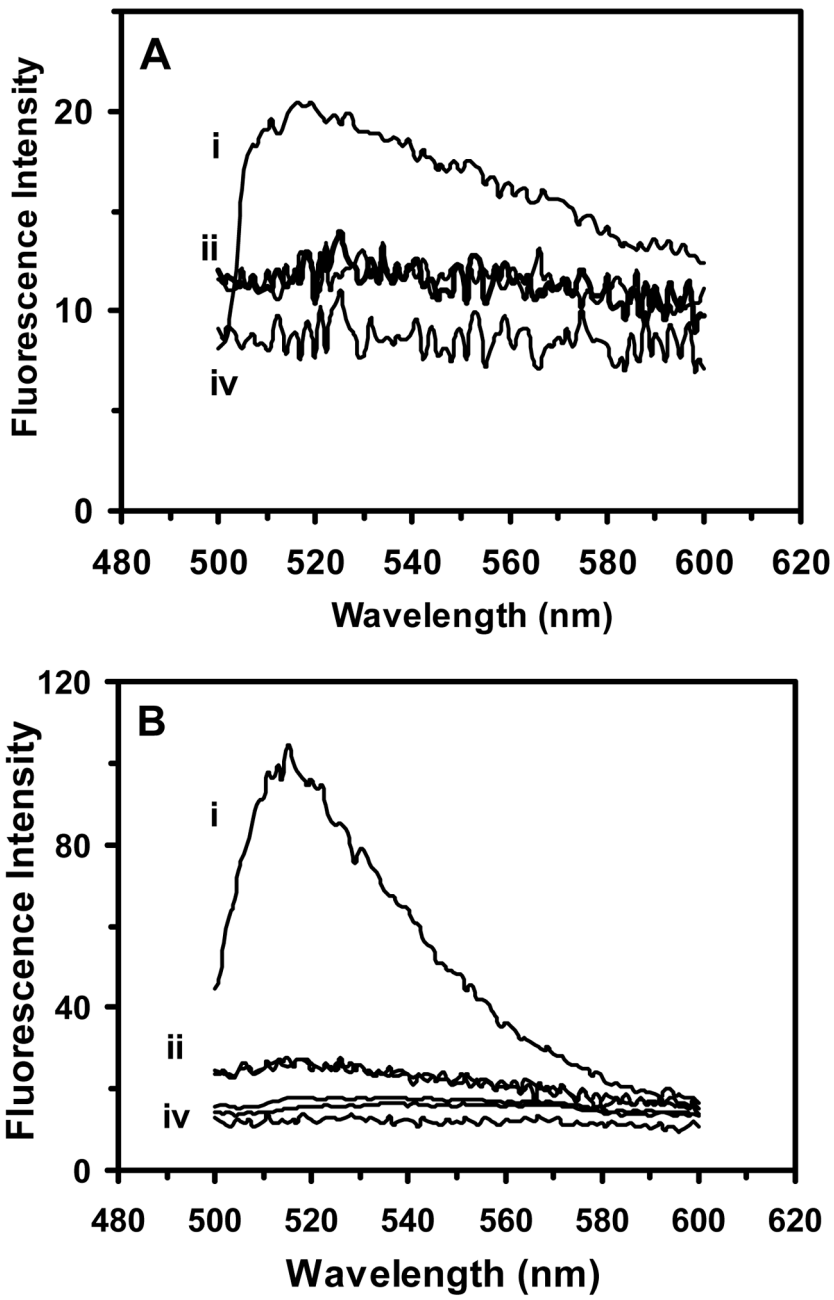

Figure 6.

Quenching effect of single Ag NPs upon the fluorescence intensity of EGFP over time. **(A)** fluorescence spectra of EGFP near the NP taken at every 30 min over their incubation (i–iv) show that the fluorescence intensity is much lower than the one in the absence of NPs in **(B)** and emission intensity decreases rapidly over time; **(B)** fluorescence spectra of EGFP alone (control experiment: in the absence of NPs) taken at every 30 min (i–iv) show significant higher fluorescence emission intensity at the initial measurement in (i) than those in (A), and fluorescence emission intensity decreases over time in (ii–iv) due to photobleaching.

Table I

Summary of LSPR Spectra of Single Ag NPs Upon Their Incubation with EGFP over Time

Incubation Time (min)	λ_{max} (nm) Single Blue NPs			λ_{max} (nm) Single Green NPs			λ_{max} (nm) Single Red NPs		
	a	b	c	a	b	c	a	b	c
0	466	488	494	506	527	536	613	650	657
90	466	488	494	506	527	536	584	626	620
180	466	488	494	506	527	536	553	608	599
$\Delta\lambda_{max}$ (nm)	0	0	0	0	0	0	60	42	58

Nanoscale. Author manuscript; available in PMC 2016 November 14.